Electron depletion at InAs free surfaces: Doping-induced acceptorlike gap states

L. F. J. Piper, T. D. Veal, M. J. Lowe,* and C. F. McConville†
Department of Physics, University of Warwick, Coventry, CV4 7AL, United Kingdom
(Received 8 July 2005; revised manuscript received 13 April 2006; published 23 May 2006)

For almost all *n*-type zinc-blende III-V semiconductor free surfaces a depletion layer is observed. InAs is an exception, since *n*-type InAs free surfaces exhibit electron accumulation, due to donorlike surface states which pin the Fermi level far above the conduction band minimum. High-resolution electron-energy-loss spectroscopy (HREELS) has been used to investigate the free surfaces of slightly degenerate ($n \sim 2 \times 10^{17}$ cm^{-3}) and highly degenerate ($n \sim 5 \times 10^{18}$ cm^{-3}) InAs. From HREEL studies of these InAs samples, an electron accumulation and depletion layer were observed, respectively. The Fermi-level pinning mechanism at free surfaces is discussed in terms of the position of the bulk Fermi level with respect to the branch-point energy (E_B). Depending on the location of the bulk Fermi level, amphoteric defects are incorporated into the surface, which if ionized facilitate the band bending that results in the surface Fermi level becoming pinned close to E_B. Occupied cation-on-anion antisite defects and unoccupied anion-on-cation antisite defects at the surface are considered to be the ionized surface states responsible for the depletion and accumulation layer profiles, respectively.

DOI: 10.1103/PhysRevB.73.195321 PACS number(s): 73.20.At, 68.47.Fg, 73.20.Mf, 79.20.Kz

I. INTRODUCTION

Semiconductor interfaces such as Schottky contacts and *p-n* junctions play an important role in existing microelectronic and optoelectronic devices; understanding their properties is necessary for future device applications. At metal-semiconductor interfaces band bending occurs, resulting in the Fermi level becoming pinned with respect to the band-edges. The location of the pinning level varies between semiconductors and corresponds well to the location of the branch-point energy (E_B).[1–3] The pinning is due to a continuum of adatom-induced gap states formed at the interface, which facilitate this band bending.[4,5] The location of E_B corresponds to the crossover between predominantly donorlike and acceptorlike states and therefore has the significance of a charge-neutrality level.[3] It is expected that E_B also plays an important role in dictating the space-charge layer formed at semiconductor free surfaces. Ionized surface states (i.e., gap states) can pin the Fermi level at semiconductor free surfaces (vacuum-semiconductor interfaces).[4,5] For almost all *n*-type semiconductor surfaces, an electron depletion layer is observed [except for perfectly cleaved III-V(110) surfaces where no band bending occurs], with the Fermi level pinned within the band gap.[5] Indium arsenide is unique among zinc-blende III-V semiconductors, since an accumulation layer is observed instead.[6–8] The electron accumulation is due to evanescent, donorlike, surface states pinning the Fermi level above the conduction band minimum (CBM).[4,7] A flat band layer profile (i.e., no band bending) is observed at clean, well-cleaved *nonpolar* InAs(110) surfaces, due to its surface exhibiting the same relaxation as GaAs(110).[9,10] However, electron accumulation is observed when either a small number of defects are introduced to,[11] or hydrogen is adsorbed on[12] the surface of lowly doped *n*-type nonpolar InAs. To date, electron depletion has never been observed at InAs free surfaces.

Here, we have employed high-resolution electron-energy-loss spectroscopy (HREELS) to investigate the near-surface space-charge profiles of InAs free surfaces to highlight the importance of the location of the bulk Fermi level with respect to E_B. HREEL studies of lowly degenerate *n*-type InAs(100)-(4×2) free surfaces revealed an accumulation layer profile consistent with previous studies.[7,13] This is in stark contrast with highly degenerate *n*-type InAs(110)-(1×1) free surfaces, where a depletion layer was observed. Although the presence of a depletion layer is initially surprising, it can be understood in terms of the bulk Fermi level lying above E_B. In fact, the two different space-charge regions observed here are consistent with the bulk Fermi level lying below (accumulation) and above (depletion) E_B; from comparisons with other III-V semiconductors we speculate on the origin and nature of the surface (or gap) states responsible for the Fermi-level pinning mechanism at InAs free surfaces.

II. EXPERIMENTAL DETAILS

In this work two sets of InAs samples supplied by Wafertech, UK were investigated, *n*-type InAs(100) (S-doped, $n \sim 2 \times 10^{17}$ cm^{-3}) and InAs(110) samples (S-doped, $n \sim 5 \times 10^{18}$ cm^{-3}). Following insertion into the HREELS chamber, the preparation of the InAs(100) samples was achieved by small doses of low-energy hydrogen (typically <1 eV), a process referred to as atomic hydrogen cleaning (AHC). The InAs(100) samples were prepared using a two stage method involving a 5 kL dose of H* at 400 K followed by a further 20 kL dose of H* at 475 K to produce a clean As-rich (2×4) reconstruction. Following the clean, the surface was dosed with sulphur using an electrochemical cell for investigating the sulphur-induced electron accumulation (reported elsewhere[13]). The sulphur was fully desorbed after annealing at 675 K and produced an In-rich (4×2) reconstruction, as shown by the LEED pattern in Fig. 1(a).

The surface preparation of the InAs(110) samples consisted of an initial clean at 335 K with 15 kL dose of H*

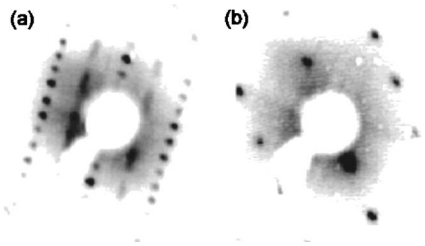

FIG. 1. The LEED patterns observed following cleaning cycles of the (a) InAs(100)-(4×2) (b) InAs(110)-(1×1) reconstructed surfaces recorded at incident electron energies of 57.7 eV and 49.0 eV, respectively.

followed by a further 15 kL dose of H^* at 575 K and a final anneal at 625 K for 10 minutes. Sharp (1×1) LEED patterns, indicating well-ordered surfaces, were observed after cleaning as shown in Fig. 1(b). The removal of atmospheric contaminants for both sets of samples was confirmed using HREELS, by the absence of vibrational modes associated with adsorbed hydrocarbons and native oxides. The adsorption of hydrogen is known to result in the formation of an accumulation layer at InAs(110) surfaces.[12] After the AHC, the HREEL spectra contained no In-H (205 meV) or As-H (260 meV) vibrational modes,[14] indicating that any hydrogen adsorbed during the AHC was completely desorbed during the anneal.

III. HREEL SPECTRA

In HREELS, a monoenergetic beam of electrons interacts with electric fields extending into the vacuum originating within the sample and the scattered electrons are energy analyzed. The majority of the probing electrons are elastically scattered, giving rise to an intense peak at zero loss energy. Other energy-loss features in the spectra are associated with the energy exchange between the fields arising from collective excitations of the conduction electrons and the lattice, with the electric fields due to the inelastically scattered electrons. The electric fields from the excitations decay exponentially into the vacuum in the form, $\exp(-q_{\|}z)$, where $q_{\|}$ is the wave-vector transfer parallel to the surface and z is the depth of the excitation. By varying the kinetic energy of the probing electrons, the inverse of the wave-vector transfer parallel to the surface is changed, thus enabling the probing depth to be varied.[7,15] Consequently, varying the probing energy of the incident electrons allows the electronic properties of the entire space-charge region to be investigated.

The energy loss of the conduction band electron plasmon is related to the carrier concentration. The dispersion of the plasmon peak as the kinetic energy is varied indicates the electron density profile close to the surface. Naively, the plasmon peak energy will shift towards higher (lower) energies with increasing probing energy for depletion (accumulation) layers. However, the situation is further complicated by spatial dispersion, which shifts the plasmon peak to higher energies with decreasing probing energy. Also, the plasmon and phonon can interact if they lie in close proximity, resulting in the formation of a coupled mode, known as a plasmaron.

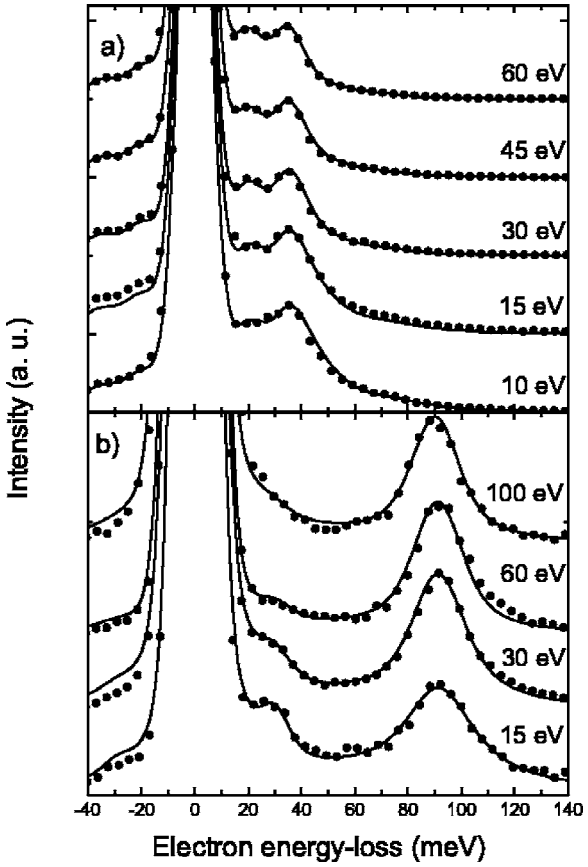

FIG. 2. The HREEL spectra (points) from the clean (a) InAs(100)-(4×2) surface and (b) InAs(110)-(1×1) surface, for a range of probing energies are shown, vertically offset. The corresponding semiclassical dielectric simulations (lines), for each incident energy, are also shown.

Figure 2(a) displays the HREEL spectra recorded from the InAs(100)-(4×2) surface, for a range of incident energies. Here, the proximity of the Fuchs-Kliewer phonon frequency (29 meV) (Ref. 16) to the conduction band plasmon frequency has resulted in the formation of a plasmaron. The presence of the plasmaron requires semiclassical dielectric theory simulations of the spectra in order to investigate the near-surface profile. The spectra obtained from the InAs(110)-(1×1) surface are shown in Fig. 2(b). Here the Fuchs-Kliewer phonon and plasmon peaks are clearly distinguished and are not coupled. In this case, the plasmon peak lies at a greater energy-loss position, reflecting the higher carrier concentration of this sample compared to the InAs(100)-(4×2). The lack of a clear plasmon peak shift with increasing probing energy results from the opposing shifts due to the depletion layer profile and spatial dispersion cancelling each other out. The increasing asymmetry of the plasmon peak with decreasing incident energy further supports this explanation.

The corresponding dielectric theory simulations of the HREEL spectra, for each incident energy, are also shown in Figs. 2(a) and 2(b). The HREEL simulations were calculated using a wave-vector-dependent dielectric function, as described by Lambin *et al.*[17,18] In this model, the solid at the

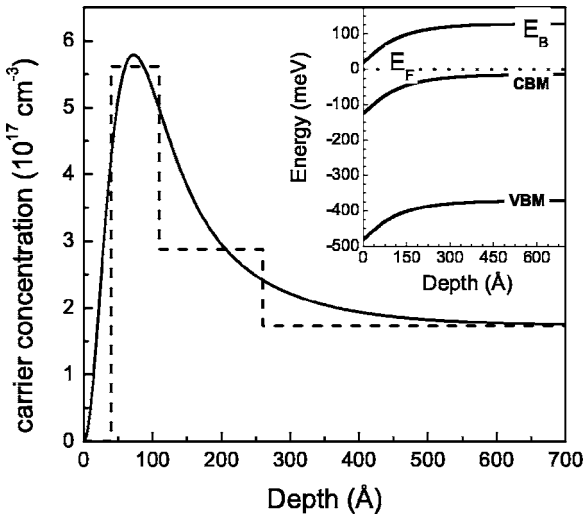

FIG. 3. The translated histogram HREEL layer profile (dashed line) and corresponding smooth Poisson-MTFA solutions (solid line) for the InAs(100)-(4×2) surface. When the bulk Fermi level lies below the branch-point energy (E_B), an electron accumulation layer profile is observed. The inset plots the resultant downward band bending of the valence band maximum, conduction band minimum, and E_B, with respect to the Fermi level (E_F).

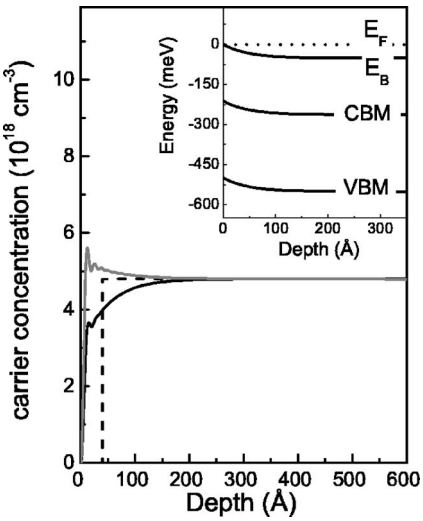

FIG. 4. The translated histogram HREEL layer profile (dashed line) and corresponding smooth Poisson-MTFA solutions for a flat band scenario (solid gray line) and a depletion layer case (solid black line) for InAs(110)-(1×1) surface are shown. A depletion layer is considered to best represent the HREEL layer profile, consistent with the bulk Fermi level (E_F) lying above the branch-point energy (E_B). Close to the surface (z∼10 Å) a feature associated with constructive interference between the electron wave functions is observed for both calculations. The inset plots the resultant upward band bending of the valence band maximum, conduction band minimum, and E_B with respect to E_F.

surface is approximated by a few thin layers on top of a bulk layer. Each layer is described by its own individual dielectric function and thickness. An effective dielectric function is then calculated from the layer contributions and is then used to simulate the spectra.

Two unique layer profiles were used to simulate all of the spectra shown in Figs. 2(a) and 2(b). For the InAs(100)-(4×2) surface, a 40 Å dead layer, followed by two further layers above a bulk layer were required. The larger plasmon energy required in the second and third layers compared to the bulk layer is consistent with the accumulation of charge near the surface. The dead layer was required to account for the quantized nature of the electron wave functions, resulting from the potential barrier formed at the surface, which suppresses the carrier concentration close to the surface.[7] An accumulation layer profile is immediately ruled out for the InAs(110)-(1×1) surface since a two-layer profile was required.

IV. ANALYSIS

The HREEL layer profiles used in the semiclassical dielectric simulations were translated from plasmon frequencies into carrier concentrations. The narrow band gap of InAs [0.356 meV at 300 K (Ref. 19)] means the nonparabolicity of the conduction band needs to be considered in any calculation. Here, the α-approximation model was used to describe the conduction band dispersion,[20] using the parameters cited in the recent review of III-V parameters by Vurgaftman *et al.*[19] The two translated HREEL layer profiles, used to simulate the spectra of the two surfaces, are shown in Figs. 3 and 4.

To complicate the situation further, conduction band renormalization effects due to electron-electron and electron-ionized impurity interactions [previously studied in highly *n*-type Si and Ge (Ref. 21)] cannot be neglected when investigating the highly degenerate *n*-type InAs(110)-(1×1) surface, due to the high bulk carrier concentration of the material. Such effects have been shown to be significant in degenerately doped InN,[22] a material similar to InAs with a nonparabolic conduction band and intrinsic electron accumulation at its surface.[23] The resultant band gap shrinkage, due to the conduction band renormalization, has been fully incorporated into the α approximation used to calculate the nonparabolic conduction band dispersion.

To validate our calculations, we referred to Hall measurements of InAs samples irradiated by high-energy protons by Brudnyĭ *et al.*[24] Their work revealed that the carrier concentration stabilized at $n=2.6\times10^{18}$ cm^{-3},[24] which corresponds to the bulk Fermi level lying at E_B.[25] Any further irradiation results in the formation of compensating amphoteric defects that ensure that the Fermi level remains stabilized at E_B, as described by the amphoteric defect model.[26] The positions of the band edges with respect to E_B (or Fermi stabilization level) have been shown to be important for understanding the electronic properties of a semiconductor.[27] This is discussed further, but for now we comment that E_B lies 0.500 eV above the valence band maximum (VBM) for InAs, derived using real-space Green function methods and empirical tight-binding calculations.[3,28] A high-energy irradiation stabilized carrier concentration of $n=2.6\times10^{18}$ cm^{-3} reported by Brudnyĭ *et al.*,[24] corresponds to a Fermi level of 0.198 eV above the CBM with a renormalized band gap of 0.301 eV, in our calculations. Therefore, the calculated Fermi level of

0.499 eV above the VBM from the Hall measurements is in excellent agreement with the 0.500 eV expected.

Incorporating the effects of nonparabolicity in calculating space-charge profiles has been shown to be necessary for InAs.[9] Here, realistic smooth charge profiles were calculated by solving the Poisson equation within the modified Thomas-Fermi approximation (MTFA). The MTFA correction reduces the carrier concentration to zero at the surface and describes the interference between the incoming electron waves and those reflected at the surface potential barrier.[29] This allows the nonparabolicity to be incorporated straightforwardly compared to the complications associated with appropriately modifying the Schrödinger equation. Such an approach has previously proved successful in describing the accumulation profiles of both InAs (Ref. 13) and InN.[30] The corresponding Poisson-MTFA solutions for the two translated HREEL layer profiles are shown in Figs. 3 and 4, for the lowly and highly degenerate *n*-type InAs samples, respectively.

A. InAs(100)-(4×2)

In Fig. 3 an accumulation layer profile is observed with a downward band bending of 0.110 eV, pinning the Fermi level at 0.481 eV above the VBM, facilitated by a donorlike surface state density of 5.83×10^{11} cm^{-2} in agreement with previous studies.[7] The inset plots the corresponding band bending as a function of depth; the Fermi level tends towards E_B at the surface. The Poisson-MTFA used to solve the space-charge region has a characteristic length term (L), which corresponds to the minimum space for a particle determined by $\Delta z\Delta p\sim\hbar$, where $\Delta z=L$ and Δp is the change in momentum of the particle.[31] This length corresponds to the radius of the bulk plasmon, i.e., the de Broglie wavelength.[32] The bulk carrier concentration of the InAs(100)-(4×2) corresponds to a Fermi level 0.015 eV above the CBM. In the calculations, $L=1/k_F$ [where k_F is the Fermi wave-vector and is given by $k_F=(3\pi^2n)^{1/3}$] has been appropriately used as required for a degenerate semiconductor. For this carrier concentration, $L=57$ Å and corresponds well to the distance between zero electron density at the surface to the peak of electron accumulation, as shown in Fig. 3. The amount of band bending required within the Poisson-MTFA of the InAs(100)-(4×2) corresponds to a pinned Fermi level of 0.481 eV above the VBM at the surface.

B. InAs(110)-(1×1)

Figure 4 displays the translated HREEL layer profile required to simulate the HREEL spectra, consisting of a 40 Å thick layer of zero plasma frequency. The Poisson-MTFA solution for the depletion layer (assuming the Fermi level tends to E_B at the surface) is presented in Fig. 4. For further comparison with the HREEL layer profile, the Poisson-MFTA solution for the flat band case (i.e., an ionized surface state density of zero) is also shown in Fig. 4; the calculated electron density profile is consistent with the description by Appelbaum and Baraff.[33] Although both the dead layer and depletion region describe the reduction of the electron concentration close to the surface, they are distinguishable as shown by Ritz and Lüth.[34] For flat band and accumulation profiles, the dead layer corresponds to a region of uncompensated donors localized at the surface.[33] The dead layer is typically found to be roughly $L/2$ for HREEL layer simulations of accumulation (as seen in Fig. 3) and flat band space-charge regions. For $n=4.8\times10^{18}$ cm^{-3} the bulk Fermi level is 0.263 eV above the CBM, which yields $L=19.2$ Å for $n=4.8\times10^{18}$ cm^{-3} with a dead layer width of ~10 Å. Here, a 40 Å width layer of zero plasma frequency is required to simulate the spectra, which is far larger than the ~10 Å necessary to approximate the flat band profile (as shown in Fig. 4). Instead, the HREEL layer profile is considered to represent the two-layer description of the depletion layer solution (refer to Fig. 4). For a degenerate semiconductor it is necessary to use a Thomas-Fermi screening length (λ_{TF}) rather than thermal screening length for the depletion layer.[35] For $n=4.8\times10^{18}$ cm^{-3}, $\lambda_{TF}=48$ Å and agrees with 40 Å required by the HREEL layer profile to simulate the spectra. Therefore, a depletion layer profile rather than a flat band case is concluded to be present at the highly degenerate *n*-type InAs(110)-(1×1) surface prepared by AHC. The inset of Fig. 4 displays the corresponding 50 meV upward band bending, driven by the 1.04×10^{11} cm^{-2} acceptorlike surface states, for the Poisson-MTFA depletion layer solution. The upward band bending results in the Fermi level being pinned at 0.502 eV above the VBM, i.e., close to E_B.

V. DISCUSSION

At semiconductor free surfaces, the Fermi-level pinning mechanism is driven by a small number of ionized surface states, referred to as gap states.[4,5] Such states arise from the termination of the bulk crystal at the surface and merely describe the spatially localized surface wave functions; these wave functions satisfy the Schrödinger equation with the requirement that they exponentially decay into the vacuum.[4,36] For instance, dangling bonds associated with a particular reconstruction represent an example of a gap state. The evanescent nature of these states is satisfied provided that their wave-vectors are complex and therefore the surface states are restricted to forbidden band gap regions. The spatially localized nature of the surface states means that their character is derived from contributions over a substantial portion of the Brillouin zone, while the Γ-point provides little in comparison.[2] States will have either predominantly valence or conduction band character corresponding to donorlike and acceptorlike states, respectively. The crossover from donorlike to acceptorlike states is referred to as E_B, which lies close to the middle of the average or dielectric gap at the mean-value point.[2,3] Charge neutrality is satisfied when all donorlike states are occupied and all acceptorlike states are empty, and occurs ideally when the Fermi level lies at E_B. However, the large screening lengths of these surface states combined with their discrete rather than continuous nature means that the Fermi-level pinning can occur away from E_B.[1]

We assert that the location of the bulk Fermi level with respect to E_B chiefly determines the space-charge profile observed. The location of E_B can be estimated using

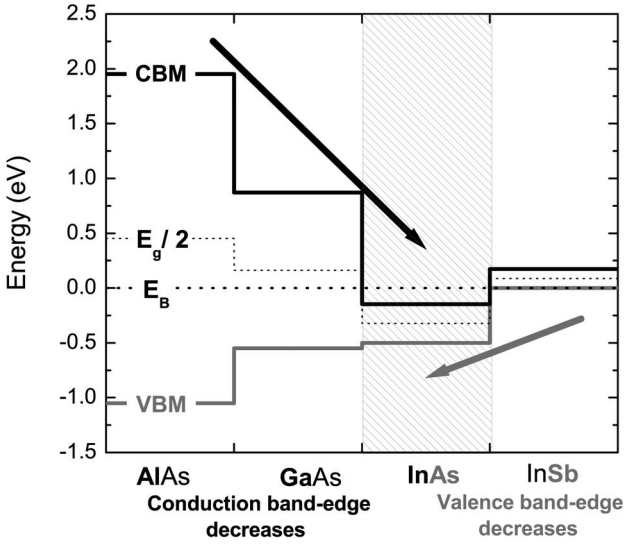

FIG. 5. The band line-up of AlAs, GaAs, InAs, and InSb referenced to the calculated positions of the branch-point energy (E_B) (solid thin line) (Refs. 2 and 3) using band parameters from the III-V review by Vurgaftman *et al.*(Ref. 19) Also shown is the midgap ($E_g/2$) position of each of the semiconductors (dotted thin line). The cation acts to push the CBM downwards, while as the spin-orbit splitting increases the VBM is pushed upwards. InAs (highlighted) represents an extreme point in the band line-up since its CBM lies below E_B and its low location is responsible for free surface electron accumulation and proclivity to *n*-type conductivity.

$$E_B \approx \tfrac{1}{2}(\overline{E_C} + \overline{E_V}), \tag{1}$$

where

$$\overline{E_V} = E_V - \tfrac{1}{3}\Delta_{SO}, \tag{2}$$

and $\overline{E_C}$ is the indirect conduction band minimum, E_V is the VBM and Δ_{SO} is the spin-orbit splitting.[2] Typically, $E_B < E_g/2$ for most semiconductors, as shown in Fig. 5. GaAs, the archetypal compound semiconductor, provides an excellent example of the role E_B plays in the formation of the space-charge layer; *n*-type GaAs will always have a bulk Fermi level above E_B and so, if any occupied acceptorlike states exist, upward band bending will occur with charge neutrality achieved once the ultimate band bending is compensated by the remaining negatively charged acceptorlike surface states. A depletion layer is then formed at the surface with the pinned surface Fermi level lying close to E_B, which for GaAs lies close to the midgap position. When a depletion layer is not observed with *n*-type GaAs free surfaces, then flat bands occur, i.e., there is no band bending due to the absence of ionized surface states. Such a situation occurs if the bulk Fermi level lies at E_B so that no ionized states exist or for perfectly cleaved nonpolar (110) surfaces. For all compound semiconductors, the anion and cation dangling bonds have valence and conduction band character, respectively. The nonpolar surface, if perfectly cleaved, relaxes such that all of the anion and cation dangling bonds lie below the VBM and above the CBM, respectively;[10] provided that the Fermi level lies within the band gap, i.e., nondegenerate, then all of the states are neutral. However, if any imperfections exist or if the bulk Fermi level lies such that it does ionize a gap state, then a space-charge layer will form to maintain overall charge neutrality.

The location of E_B high above the CBM for InAs—as shown in Fig. 5—generally results in the formation of an accumulation layer, due to the bulk Fermi level lying below E_B. Charge neutrality is achieved when the surface Fermi level is pinned close to E_B, with the ultimate amount of downward band bending being compensated by the remaining unoccupied donorlike surface states. However, if the bulk Fermi level of InAs lies above E_B, then the situation is the same as for *n*-type GaAs and a depletion layer is expected.

It is important to note that the position of E_B is not unusually high for InAs, rather the Γ-point CBM is extremely low. In fact, there is evidence that the position of E_B is universal for all covalent and weakly ionic semiconductors, lying approximately 4.9 eV below the vacuum level.[37,38] Instead, chemical trends reveal that the CBM is particularly sensitive to the cation; by changing the cation from Al→Ga→In, the Γ-point minimum decreases, as shown in Fig. 5.[2] From this rule alone, the same phenomenon should also occur for InSb. However, the VBM is affected most by the spin-orbit splitting. Antimonides have the greatest spin-orbit splitting and this results in the Γ-point maximum lying higher than for arsenides (see Fig. 5).[2] This is the reason why E_B lies close to the VBM for InSb, while for InAs it lies above the CBM.

As previously explained, the high-energy proton irradiated InAs stabilized carrier concentration corresponds to the bulk Fermi level lying at E_B; the carrier concentration of $n=2.6\times10^{18}$ cm^{-3} reported by Brudnyĭ *et al.*,[24] means that the InAs(100)-(4×2) ($n=1.73\times10^{17}$ cm^{-3}) and the InAs(110)-(1×1) ($n=4.8\times10^{18}$ cm^{-3}) samples investigated here have bulk Fermi levels below and above E_B, respectively. Accumulation (see Fig. 3) and depletion (see Fig. 4) layers are observed when the bulk Fermi level lies below and above E_B, respectively. Furthermore, in both cases the band bending can be explained in terms of the Fermi level tending towards E_B at the surface.

This work highlights the importance of both the location of E_B and the bulk Fermi level when investigating the near-surface electronic properties of a semiconductor. Within the context of our results, it is possible to speculate on the physical origin of the surface states responsible for the universal nature of the Fermi-level pinning mechanism at free surfaces. Although one cannot rule out adatom-induced surface states—due to the presence of possible adatoms (e.g., oxygen and hydrogen) below our detection limit—the surface states are likely to be associated with states intrinsic to the semiconductor, e.g., defects. To support this claim, we refer to the remarkable agreement between studies of InAs grown by molecular beam epitaxy, characterized *in-situ* with HREELS by Noguchi *et al.*[7] and the InAs(100)-(4×2) case reported here. Also, defects are consistent with the presence of a space-charge layer observed at heavily doped *n*-type InAs(110)-(1×1) reported here; perfectly cleaved III-V(110)-(1×1) surfaces exhibit flat bands, yet space-charge formation occurs following the introduction of defects.[11] Furthermore, studies of adsorbate-induced surface states at

InAs(110)-(1×1) surfaces revealed that nondegenerately doped *p*- and *n*-type (such that $E_F<E_B$) surfaces produced inversion and accumulation layers, respectively; following continued exposure of chlorine and oxygen, the Fermi level became pinned at 0.52 eV above the VBM for both cases, suggesting that the physical origin of the adsorbate-induced surface state is the same and must be related with defects which are not adsorbate specific.[39]

The remainder of this section focuses on the striking correlation between Fermi-level pinning in heavily irradiated semiconductors and at metal-semiconductor interfaces reported by Walukiewicz,[25] within the context of our findings of the Fermi-level dependence of the type of surface state (whether acceptorlike or donorlike). It is known that the formation energies of the donorlike (acceptorlike) defect complexes decrease as the bulk Fermi level increases (decreases) with respect to E_B, according to the amphoteric defect model.[26] We consider these amphoteric defects, when localized at the surface, are the gap states responsible for the Fermi-level pinning, such that if the Fermi level lies above (below) E_B, the creation of acceptorlike (donorlike) defect complexes at the surface becomes energetically favorable. To highlight this, we refer to positron annihilation studies of GaAs where *p*-type material (bulk Fermi level $<E_B$) formed anion vacancies and anion on cation antisite (AAS) defect complexes of donorlike character; and *n*-type material (bulk Fermi level $>E_B$) created cation vacancies and cation on anion antisite (CAS) defect complexes of acceptorlike nature.[25,26]

Antisite defects have previously been considered as the surface state responsible for the Fermi-level pinning mechanism, from comparisons of experimental results and tight-binding calculations.[40] In other studies, the CAS defect, with largely conduction band character, is considered to be the acceptorlike surface state responsible for pinning the Fermi level at most *n*-type III-V surfaces.[41] Such a situation requires that some of the CAS defects are occupied in order to be negatively charged, otherwise they would be neutral.[4] For most III-V semiconductors this appears plausible, except for *n*-type InAs where donorlike surface states are generally observed. Olssön *et al.* suggested that the source of the donorlike surface states was CAS defects, as suggested by Pötz and Ferry.[41] However, these states would only ever be either neutral or negatively charged. Instead, we attribute the donorlike surface states to unoccupied dangling bonds of the AAS defect, with largely valence band character, which would be positively charged. The downward band bending is then facilitated by the transfer of electrons to the conduction band from a small number of ionized antisite defects (typically of the order of $\sim10^{12}$ cm^{-2}). By analogy, it is likely that the occupied CAS and unoccupied AAS are the acceptorlike and donorlike surface states responsible for the Fermi-level pinning, respectively, with the location of the bulk Fermi level with respect to E_B determining the likelihood of each type of defect at the surface.

VI. CONCLUSION

The Fermi-level pinning mechanism at semiconductor free surfaces is discussed in terms of the position of the bulk Fermi level with respect to E_B. From HREEL studies of InAs, an electron depletion and accumulation layer were observed when the bulk Fermi level was above and below E_B, respectively. Depending on the location of the bulk Fermi level, amphoteric defects are incorporated into the reconstruction, which if ionized facilitate the band bending that results in the surface Fermi level becoming pinned close to E_B. Occupied CAS and unoccupied AAS defects at the surface are considered to be the ionized surface states responsible for the depletion and accumulation layer profiles, respectively.

*Current address: National Physical Laboratory, Hampton Road, Teddington, Middlesex TW11 0LW, United Kingdom.
†Electronic address: c.f.mcconville@warwick.ac.uk

[1] J. Tersoff, Phys. Rev. Lett. **52**, 465 (1984).
[2] J. Tersoff, Phys. Rev. B **32**, 6968(R) (1985).
[3] W. Mönch, J. Appl. Phys. **80**, 5076 (1996).
[4] W. Mönch, *Semiconductor Surfaces and Interfaces* (Springer, Berlin, 1993).
[5] W. Mönch, Rep. Prog. Phys. **53**, 221 (1990).
[6] D. C. Tsui, Phys. Rev. Lett. **24**, 303 (1970).
[7] M. Noguchi, K. Hirakawa, and T. Ikoma, Phys. Rev. Lett. **66**, 2243 (1991).
[8] L. Ö. Olsson, C. B. M. Andersson, M. C. Hakansson, J. Kanski, L. Ilver, and U. O. Karlsson, Phys. Rev. Lett. **76**, 3626 (1996).
[9] S. Abe, T. Inaoka, and M. Hasegawa, Phys. Rev. B **66**, 205309 (2002).
[10] H. Cartensen, R. Claessen, R. Manzke, and M. Skibowski, Phys. Rev. B **41**, 9880 (1990).
[11] H. S. Karlsson, G. Ghiaia, and U. O. Karlsson, Surf. Sci. **407**, L687 (1998).
[12] Y. Chen, J. C. Hermanson, and G. J. Lapeyre, Phys. Rev. B **39**, 12682 (1989).
[13] M. J. Lowe, T. D. Veal, A. P. Mowbray, and C. F. McConville, Surf. Sci. **544**, 320 (2003).
[14] Y. Chen, Ph.D. thesis, Montana State University, Boseman Montana, 1999.
[15] T. S. Jones, M. O. Schweitzer, N. V. Richardson, G. R. Bell, and C. F. McConville, Phys. Rev. B **51**, 17675 (1995).
[16] R. Fuchs and K. L. Kliewer, Phys. Rev. **140**, A2076 (1965).
[17] Ph. Lambin, J. P. Vigneron, and A. A. Lucas, Comput. Phys. Commun. **60**, 351 (1990).
[18] Ph. Lambin, J. P. Vigneron, and A. A. Lucas, Phys. Rev. B **32**, 8203 (1985).
[19] I. Vurgaftman, J. R. Meyer, and L. R. Ram-Mohan, J. Appl. Phys. **89**, 5815 (2001).
[20] B. R. Nag, *Electron Transport in Compound Semiconductors* (Springer, Berlin, 1980).
[21] K. F. Berggren and B. E. Sernelius, Phys. Rev. B **24**, 1971 (1981).
[22] J. Wu, W. Walukiewicz, K. M. Yu, J. W. Ager III, E. E. Haller, H.

Lu, and W. J. Schaff, Phys. Rev. B **66**, 201403(R) (2002).
[23] I. Mahboob, T. D. Veal, C. F. McConville, H. Lu, and W. J. Schaff, Phys. Rev. Lett. **92**, 036804 (2004).
[24] V. N. Brudnyĭ, N. G. Kolin, and A. I. Potapov, Semiconductors **37**, 408 (2003).
[25] W. Walukiewicz, Phys. Rev. B **37**, 4760 (1988).
[26] W. Walukiewicz, Appl. Phys. Lett. **54**, 2094 (1989).
[27] W. Walukiewicz, Physica B **302**, 123 (2001).
[28] J. Tersoff, Surf. Sci. **168**, 275 (1986).
[29] J. P. Zöllner, H. Übensee, G. Paasch, T. Fiedler, and G. Gobsch, Phys. Status Solidi B **134**, 837 (1986).
[30] L. F. J. Piper, T. D. Veal, I. Mahboob, C. F. McConville, H. Lu, and W. J. Schaff, Phys. Rev. B **70**, 115333 (2004).
[31] G. Paasch and H. Übensee, Phys. Status Solidi B **113**, 165 (1982).
[32] I. Egri, R. Matz, H. Lüth, and A. Stahl, Surf. Sci. **128**, 51 (1983).
[33] J. A. Appelbaum and G. A. Baraff, Phys. Rev. Lett. **26**, 1432 (1971).
[34] A. Ritz and H. Luth, J. Vac. Sci. Technol. B **3**, 1153 (1985).
[35] Z. J. Gray-Grychowski, R. G. Egdell, B. A. Joyce, R. A. Stradling, and K. A. Woodbridge, Surf. Sci. **186**, 482 (1987).
[36] H. Luth, *Surfaces and Interfaces of Solid Materials* (Springer, Berlin, 1995).
[37] J. Wu and W. Walukiewicz, Superlattices Microstruct. **34**, 63 (2003).
[38] J. Tersoff and W. A. Harrison, Phys. Rev. Lett. **58**, 2367 (1987).
[39] K. Smit, L. Koenders, and W. Mönch, J. Vac. Sci. Technol. B **7**, 888 (1989).
[40] R. Allen and J. D. Dow, Phys. Rev. B **25**, 1423 (1982), and references therein.
[41] W. Pötz and D. K. Ferry, Phys. Rev. B **31**, 968 (1985).